Multimodality Nuclear and Fluorescence Tumor Imaging in Mice Using a Streptavidin Nanoparticle

Minmin Liang,[†,‡] Xinrong Liu,[†] Dengfeng Cheng,[†] Guozheng Liu,[†] Shuping Dou,[†] Yi Wang,[†] Mary Rusckowski,[†] and Donald J. Hnatowich*[,†]

Department of Radiology, University of Massachusetts Medical School, Worcester, Massachusetts 01655, and National Laboratory of Biomacromolecules, Institute of Biophysics, Chinese Academy of Sciences, 15 Datun Road, Beijing 100101, China. Received February 9, 2010; Revised Manuscript Received May 17, 2010

Combining two or more different imaging modalities in the same agent can be of considerable value in molecular imaging. We describe the use of streptavidin nanoparticle-based complexes as multimodality imaging agents to achieve tumor detection in a mouse model by both fluorescence and nuclear imaging. Up to four biotinylated functionalities can be readily attached to these streptavidin nanoparticles without apparent influence on their properties and with reasonable pharmacokinetics and therefore may be ideally suited for multimodality imaging. By binding a biotinylated anti-Her2 Herceptin antibody to provide tumor targeting, a biotinylated DOTA chelator labeled with ^{111}In and a biotinylated Cy5.5 fluorophore to a streptavidin nanoparticle, we demonstrated multimodality imaging in SUM190 (Her2+) tumor bearing mice on both an IVIS fluorescence camera and a NanoSPECT/CT small animal nuclear camera. The imaging results show high tumor accumulation and strong tumor-to-normal tissue contrast by both fluorescence and nuclear imaging. The subsequent biodistribution study confirmed the specific tumor accumulation in that tumor accumulation of radioactivity at 40 h was 21 ID%/g and therefore much higher than all other tissues including liver, heart, kidney, spleen, and muscle that accumulated 8.7, 2.5, 6.9, 7.2, and 1.9 ID%/g, respectively. In conclusion, the streptavidin nanoparticle under development in this laboratory was used effectively for multimodality imaging of tumor in mice by fluorescence and nuclear detection. Presumably, other imaging modalities could also be considered.

INTRODUCTION

Optical imaging is a relatively new imaging modality that provides rapid, low-cost, and real-time screening for surface lesions such as breast cancer (*1*−*3*). However, optical imaging suffers from limited sensitivity with tissue depth due to light absorption and scatter and as yet has limited ability to provide quantitative and tomographic information (*4*−*7*). By contrast, nuclear imaging offers excellent sensitivity regardless of tissue depth and readily provides both tomographic as well as quantitative information but at a considerably higher cost (*8*−*10*). Thus, the coupling of nuclear and optical imaging in the same agent could overcome the shortcomings of each and combine the benefits of each modality.

In the past several years, many conjugates have been developed by integrating antibodies, peptides, ligands, gene complexes, or small molecule probes with radioactive and optical agents using covalent conjugation (*11*−*15*). This laboratory is developing a nanoparticle based on streptavidin to which up to four biotinylated functionalities can be readily attached without apparent influence on their properties and with reasonable pharmacokinetics (*16*−*18*). The nanoparticle therefore appears to be ideally suited for multimodality imaging. In this study, we developed a trifunctional dual-modality nanoparticle to achieve tumor detection in a mouse model by both fluorescence and nuclear imaging. The nanoparticle consisted of the biotinylated anti-Her2 Herceptin antibody to provide tumor targeting, a biotinylated DOTA chelator labeled with ^{111}In and a biotinylated Cy5.5 fluorophore, each linked via streptavidin. The antitumor antibody, Herceptin, binds to the extracellular segment of the Her2 receptor and is widely used in the clinic in combination with chemotherapy to increase both survival and response rate in breast cancer patients (*19*−*22*). The streptavidin nanoparticles are easily prepared by simple mixing and therefore allow ready replacement of functionalities on the streptavidin core. To our knowledge, no streptavidin-based dual-modality nuclear-fluorescence imaging agents have been reported.

MATERIALS AND METHODS

Chemicals. The clinical-grade anti-Her2 antibody trastuzumab (Herceptin) was manufactured by Genentech, Inc. (South San Francisco, CA, USA). The *N*-hydroxysuccinimide ester of Cy5.5 (NHS-Cy5.5) was obtained from GE Healthcare (Piscataway, NJ). The biotinylation reagent biocytin was from Sigma (St. Louis, MO, USA) and used to biotinylate NHS-Cy5.5; sulfosuccinimidyl-6-[biotinamido]-6-hexanamido hexanoate (sulfo-NHS-LC-LC-biotin) was from Pierce (Rockford, IL, USA) and used to biotinylate Herceptin. The streptavidin was purchased from Sigma (St. Louis, MO, USA). The human breast cancer cell line SUM190 (Her2+) was obtained from Asterand Co. (Detroit, MI, USA) and was grown in Ham's F-12 medium with 5 μg/mL insulin, 1 μg/mL hydrocortisone, 5 mM ethanolamine, 5 μg/mL transferrin, 10 nM triiodothyronine, 50 nM sodium selenite, and 1 g/L bovine serum albumin. The biotinylated DOTA derivative was obtained from Macrocyclics Inc. (Dallas, TX, USA) and $^{111}InCl_3$ was from Perkin-Elmer Life Science Inc. (Boston, MA, USA). All other chemicals were of reagent grade and used without purification.

Size-exclusion HPLC analyses were performed on a Superose 12 (Amersham Pharmacia Biotech, Piscataway, NJ, USA) installed on a Waters 515 solvent delivery system (Waters, Milford, MA, USA) equipped with an in-line radioactivity detector and a Waters UV2487 dual wavelength absorbance

[†] University of Massachusetts Medical School.
[‡] Institute of Biophysics, Chinese Academy of Sciences.

10.1021/bc100081h
Published on Web 06/17/2010

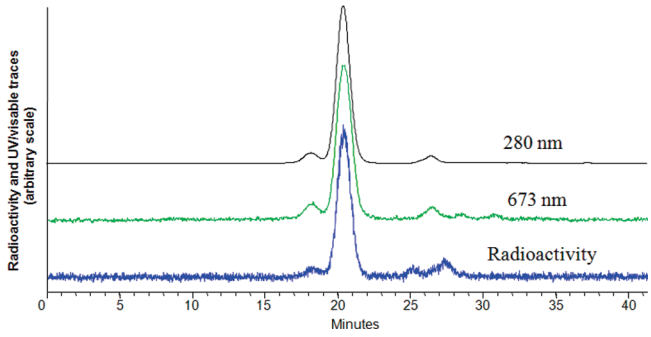

Figure 1. Size-exclusion HPLC traces of the Cy5.5/streptavidin/DOTA-^{111}In nanoparticle by in-line UV detection at 280 nm (streptavidin) and 673 nm (Cy5.5) and radioactivity detection.

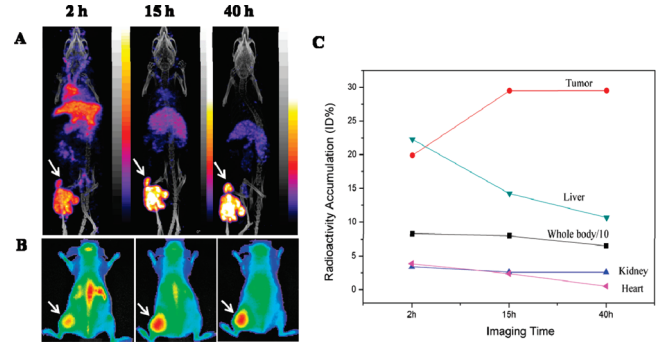

Figure 2. In vivo imaging of a representative tumored mouse at 2, 15, and 40 h post-administration of the Cy5.5/Herceptin/DOTA-^{111}In nanoparticle by SPECT/CT (A) and fluorescence imaging (B). Arrows mark the tumor location. Also presented is radioactivity quantitation by imaging in percent injected dose (%ID) in tumor, liver, kidney, heart, and whole body (C).

detector. The running solution was 20% acetonitrile in 0.1 M Tris-HCl, pH 8.0, at a flow rate of 0.6 mL/min.

Biotinylation of Herceptin Antibody. Herceptin from a reconstituted commercial vial was purified from histidine by dialyzing against 0.1 M $NaHCO_3$ solution, pH 8.5, overnight. The dialyzed Herceptin was added to a nonstick microfuge tube containing sulfo-NHS-LC-LC-biotin at a molar ratio of Herceptin to sulfo-NHS-LC-LC-biotin of approximately 1:4.6. The longer LC-LC linker was used in the antibody conjugation in place of the shorter LC linker to help avoid steric hindrance when bound to streptavidin. The preparation was mixed by gentle agitation for 1 h at room temperature and then dialyzed again against phosphate-buffered saline (PBS) overnight. The conjugated antibody was stored in PBS at 4 °C.

Labelings and Nanoparticle Preparations. The NHS-Cy5.5 was biotinylated by the following procedure. The NHS-Cy5.5 was dissolved in dry dimethylformamide and added to biocytin in 0.1 M $NaHCO_3$, pH 8.5, at a 10-fold molar excess to ensure that free biocytin was effectively consumed. The solution was gently vortexed for 1 h at room temperature in the dark and then stored overnight to hydrolyze the unreacted NHS ester on Cy5.5 to the free acid. The solution was then added very slowly and with vigorous agitation to streptavidin dissolved in 0.15 M saline at a biocytin to streptavidin molar ratio of 1:1. After 30 min of incubation in the dark, the product was purified on a polyacrylamide column (Thermo Scientific, Rockford, IL, USA, MWCO 6000) using 0.1 M PBS, pH 7.2, as eluant to remove the free Cy5.5. The Cy5.5-labeled streptavidin (Cy5.5/streptavidin) was analyzed by HPLC that showed only a single absorbance peak in the UV trace at 280 nm (streptavidin) corresponding to a single absorbance peak in the visible at 673 nm (Cy5.5). The Cy5.5 concentration was determined by measuring the absorbance at 673 nm and the concentration of streptavidin was determined using a BCA protein assay reagent kit (Pierce, Rockford, IL, USA). The Cy5.5:streptavidin molar ratio was calculated to be 1.1:1.

The preparation of the Cy5.5/streptavidin/DOTA nanoparticle was accomplished by mixing the Cy5.5/streptavidin complex with the biotinylated DOTA at a molar ratio of 1:1 with vigorous agitation for 30 min at room temperature. The $^{111}InCl_3$ stock solution in 0.05 M HCl was mixed with an equal volume of 0.5 M sodium acetate buffer, resulting in a final pH 5.5 and 500 μCi was then added to the prepared Cy5.5/streptavidin/DOTA complex and allowed to incubate at 43 °C for 1 h. The labeled product Cy5.5/streptavidin/DOTA-^{111}In was analyzed on a size-exclusion HPLC with a Superose 12 column. As shown in Figure 1, the appearance of a single peak in the UV trace at 280 nm (streptavidin) corresponding to a single peak at 673 nm (Cy5.5), and the single peak in the radioactivity trace (^{111}In) was taken as evidence of complete complexation at specific radioactivity of about 10 μCi/μg. Radioactivity recoveries were in all cases 90% or better. Finally, the biotinylated Herceptin was added and the product was incubated at room temperature for an additional 30 min in the same manner. The final Cy5.5/Herceptin/^{111}In-DOTA nanoparticle was drawn into a 1 mL U-100 insulin syringe for injection.

Animal Studies. All animal studies were performed with the approval of the UMMS Institutional Animal Care and Use Committee. Female nude mice (NIH Swiss, Taconic Farms, Germantown, NY, USA, 25−30 g) at 7 weeks of age were each injected subcutaneously in the left thigh with a 0.1 mL suspension containing 10^6 SUM190 cells mixed with 5 mg of Matrigel per milliliter. Mice were used for imaging studies 14 days later when the tumors reached 0.4−0.6 cm in diameter and were placed on a chlorophyll-free diet (AIN-93G Purified Diet, Harlan Teklad, Madison, WI) for 5 days prior to imaging.

Mice with SUM190 tumor xenografts were intravenously administered Cy5.5/Herceptin/DOTA-^{111}In nanoparticles containing 50 μg streptavidin, 139 μg Herceptin, 500 μCi of ^{111}In, and 1 nmol of Cy5.5 in 200 μL of saline. Mice were imaged on an IVIS 100 small-animal imaging system using a Cy5.5 filter set (Xenogen, Alameda, CA) at 2, 15, and 40 h post-intravenous administration under anesthesia by inhalation of oxygen−isofluorane. The mice were also imaged at approximately the same time points on a NanoSPECT/CT small animal nuclear camera (Bioscan, Washington, DC, USA) with region-of-interest (ROI) analysis using *InVivoScope 1.37* software (Bioscan). After the last image at 40 h, the mice were immediately sacrificed by cervical dislocation under anesthesia by isoflurance inhalation for biodistribution. Samples of blood and organs were removed, weighed, and counted for radioactivity in a dose calibrator.

RESULTS

Four nude mice each bearing SUM190 tumors in the left thigh received an injection of the multimodality Cy5.5/Herceptin/DOTA-^{111}In nanoparticle and were imaged on both an IVIS fluorescence scanner and a NanoSPECT/CT small animal nuclear scanner for comparison at 2, 15, and 40 h. A typical set of SPECT/CT acquisition are shown in Figure 2A, and for the same animal, a set of IVIS fluorescence images in the dorsal view at the corresponding time points are shown in Figure 2B. Figure 2C presents the percent of the injected radioactivity at each time point in several organs measured by volume of interest (VOI) analyses using *InVivoScope* software.

Figure 3 shows the biodistribution of radioactivity at 40 h postinjection. Tumor accumulation was 21 ID%/g and therefore

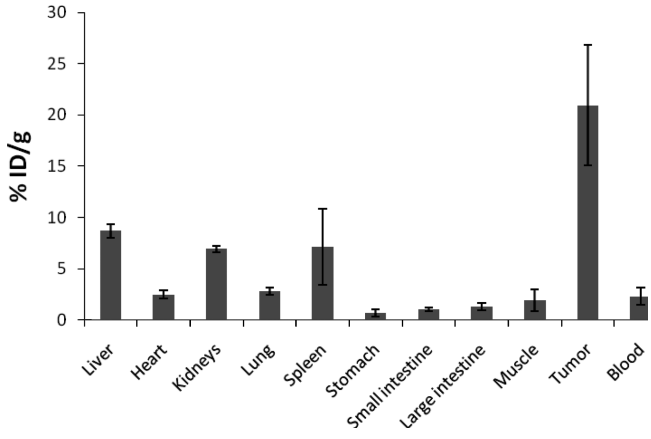

Figure 3. Biodistribution of the trifunctional multimodality nanoparticle by radioactivity (% ID/g) in tumor and selected organs at 40 h postinjection by sacrifice and dissection. ($N = 3$, error bars represent one standard deviation.)

much higher than all normal tissues such as liver, heart, kidneys, spleen, and muscle that accumulated 8.7, 2.5, 7.0, 7.2, and 1.9 ID%/g, respectively.

DISCUSSION

With the benefits of molecular imaging becoming increasingly apparent in many fields of medical research, it is also becoming increasingly apparent that no one imaging modality will serve all needs. Accordingly, an ability to couple two or more imaging modalities within the same agent could be useful. This laboratory is developing a nanoparticle based on streptavidin that is ideally suited to multimodality imaging, since up to four biotinylated functionalities can be readily combined without apparent influence on their properties and with reasonable pharmacokinetics (*16*−*18*). We had previously established that the noncovalent bond between streptavidin and biotin is sufficiently stable in vivo, that different biotinylated components (antibodies, cell penetrating peptides, DNA, and MORF oligomers) on streptavidin within the nanoparticle apparently exhibit preserved function, and that the nanoparticle exhibits favorable pharmacokinetics (*16*−*18, 25, 26*). Finally, we had previously shown that the nanoparticle is capable of accumulating in tumor by specific mechanisms. In our earliest studies, the nanoparticle was labeled with ^{99m}Tc or Cy3 and studied in SUM190 (Her2+) and SUM149 (Her2−) cells in culture (*18*). The nanoparticle accumulation was significantly higher in SUM190 vs SUM149 cells (10% vs 2% at 7 h). When the Herceptin was omitted from the nanoparticle, accumulation dropped to that of controls (<2%) and the difference in accumulation between SUM190 and SUM149 cells disappeared. The nanoparticle has also been incubated in these cells while labeled with ^{99m}Tc or Lissamine. Accumulations were again significantly higher in SUM190 vs SUM149 cells (11% vs 0.2% at 12 h) and the immunofluorescence results confirmed the much higher accumulation in the Her2+ cells (*26*). When administered to SUM190 tumor-bearing mice, accumulation reached 17%ID/g at 9 h and therefore similar to the 21%ID/g at 40 h in this multimodality study, a value that could not be achieved by any conceivable nonspecific mechanism. In a direct comparison of our nanoparticle labeled with ^{111}In with that of ^{111}In-labeled Herceptin in SUM190 tumors, both the images and the necropsy results were remarkably similar (*16*). For example, at 8 h, tumor accumulation was 10% vs 12% ID/g. In this case, the ^{111}In was on the MORF oligomer that clears rapidly through the kidneys and does not accumulate in tumor unless coupled to Herceptin. When the Herceptin is omitted from the nanoparticle, the tumor accumulation falls to about 3% ID/g at 21 h (*17*). These results show conclusively that our nanoparticle accumulates specifically in Her2+ tumors due to the presence of the Herceptin. Although not pertinent to this study, several of these reports also present results showing conclusively that accumulation is significantly higher when the nanoparticle is incubated with the radiolabeled antisense oligomer compared to the radiolabeled control oligomer, as further evidence of specific binding.

As shown in Figure 2A and B, the tumor is evident in both the fluorescent and nuclear images at all times, confirming that the streptavidin nanoparticle successfully delivered all three components to the tumor target such that each component could perform its function. The high tumor accumulation is due to the antitumor Herceptin antibody carried by the nanoparticle to the tumor, while the images are due to the nuclear and fluorescent labels also delivered to the tumor by the nanoparticle.

The nuclear images obtained on a SPECT/CT camera located the tumor with relatively high resolution (Figure 2A) and provided quantitative information on accumulations in tumor and in several normal organs (Figure 2C). Fluorescence imaging obtained on the IVIS scanner provides a relatively inexpensive and complementary approach to real-time tumor screening (Figure 2B). Despite the tissue absorption and lower resolution inherent in these fluorescent images, the two modelities have provided images that are remarkably similar and in which the tumor kinetics of the nanoparticle could have been estimated by either method with equal effectiveness.

CONCLUSION

Both the fluorescent and nuclear images confirm that each component of the Cy5.5/Herceptin/DOTA-^{111}In nanoparticle has performed as expected. The obvious accumulation in the Her2+ tumor and the impressive tumor/normal tissue ratios is a result of the presence of a functioning Herceptin within the nanoparticle. That this favorable biodistribution was observed by both fluorescence and nuclear imaging confirms that the Cy5.5 fluorophore and the ^{111}In along with its DOTA chelator remained bound to the antibody throughout the imaging period. Thus, the streptavidin nanoparticle under development in this laboratory was used effectively for multimodality imaging of tumor in mice by fluorescence and nuclear detection. Presumably, other imaging modalities could also be considered.

LITERATURE CITED

(1) Massoud, F. T., and Gambhir, S. S. (2003) Molecular imaging in living subjects: seeing fundamental biological processes in a new light. *Gene. Dev. 17*, 545–580.
(2) Liu, X., Wang, Y., Nakamura, K., Liu, G., Dou, S., Kubo, A., Rusckowski, M., and Hnatowich, D. J. (2007) Optical antisense imaging of tumor with fluorescent DNA duplexes. *Bioconjugate Chem. 18*, 1905–1911.
(3) Liang, M., Liu, X., Cheng, D., Nakamura, K., Wang, Y., Dou, S., Liu, G., Rusckowski, M., and Hnatowich, D. J. (2009) Optical antisense tumor targeting in vivo with an improved fluorescent DNA duplex probe. *Bioconjugate Chem. 20*, 1223–1227.
(4) Alfano, R. R., Demos, S. G., and Gayen, S. K. (1997) Advances in optical imaging of biomedical media. *Ann. N. Y. Acad. Sci. 820*, 248–270.
(5) Kaijzel, E. L., Pluijm, G., and Löwik, C. W. G. M. (2007) Whole-body optical imaging in animal models to assess cancer development and progression. *Clin. Cancer Res. 13*, 3490–3497.
(6) Cheng, Z., Levi, J., Xiong, Z., Gheysens, O., Keren, S., Chen, X., and Gambhir, S. S. (2006) Near-infrared fluorescent deoxyglucose analogue for tumor optical imaging in cell culture and living mice. *Bioconjugate Chem. 17*, 662–669.
(7) Ntziachristos, V., Bremer, C., and Weissleder, R. (2003) Fluorescence imaging with near-infrared light: new technological

advances that enable in vivo molecular imaging. *Eur. Radiol. 13*, 195–208.

(8) Weissleder, R., and Mahmood, U. (2001) Molecular imaging. *Radiology 219*, 316–333.

(9) Rosenthal, M. S., Cullom, J., Hawkins, W., Moore, S. C., Tsui, B. M., and Yester, M. (1995) Quantitative SPECT imaging: A review and recommendations by the focus committee of the society of nuclear medicine computer and instrumentation council. *J. Nucl. Med. 36*, 1489–1513.

(10) Chatziioannou, A. F. (2002) Molecular imaging of small animals with dedicated PET tomographs. *Eur. J. Nucl. Med. 29*, 98–114.

(11) Blasberg, G. R. (2003) in vivo molecular-genetic imaging: multi-modality nuclear and optical combinations. *Nucl. Med. Biol. 30*, 879–888.

(12) Bhushan, R. K., Misra, P., Liu, F., Mathur, S., Lenkinski, R., and Frangioni, V. J. (2008) Detection of breast cancer microcalcifications using a dual-modality SPECT/NIR fluorescent probe. *J. Am. Chem. Soc. 130*, 17648–17649.

(13) Cao, Q., Cai, W., Gang, N., He, L., and Chen, X. (2008) Multimodality imaging of IL-18-binding protein-Fc therapy of experimental lung metastasis. *Clin. Cancer Res. 14*, 6137–6145.

(14) Ponomarev, V., Doubrovin, M., Serganova, I., Vider, J., Shavrin, A., Beresten, T., Ivanova, A., Ageyeva, L., Tourkova1, V., Balatoni, J., Bornmann, W., Blasberg, R., and Gelovani, T. J. (2004) A novel triple-modality reporter gene for whole-body fluorescent, bioluminescent, and nuclear noninvasive imaging. *Eur. J. Nucl. Med. Mol. Imaging 31*, 740–751.

(15) Culver, J., Akers, W., and Achilefu, S. (2008) Multimodality molecular imaging with combined optical and SPECT/PET modalities. *J. Nucl. Med. 49*, 169–172.

(16) Liu, X., Wang, Y., Nakamura, K., Kawauchi, S., Akalin, A., Cheng, D., Chen, L., Rusckowski, M., and Hnatowich, D. J. (2009) Auger radiation-induced, antisense-mediated cytotoxicity of tumor cells using a three-component streptavidin delivery nanoparticle with 111In. *J. Nucl. Med. 50*, 582–590.

(17) Wang, Y., Liu, X., Nakamura, K., Chen, L., Rusckowski, M., and Hnatowich, D. J. (2009) In vivo delivery of antisense MORF oligomer by MORF/carrier streptavidin nanoparticles. *Cancer Biother. Radiopharm. 24*, 573–578.

(18) Liu, X., Wang, Y., Nakamura, K., Kubo, A., and Hnatowich, D. J. (2008) Cell studies of a three-component antisense MORF/tat/herceptin nanoparticle designed for improved tumor delivery. *Cancer Gene Ther. 15*, 126–132.

(19) Nahta, R., and Esteva, F. J. (2003) HER2-targeted therapy: lessons learned and future directions. *Clin. Cancer Res. 9*, 5078–5084.

(20) Piccart-Gebhart, M. J., Procter, M., Leyland-Jones, B., Goldhirsch, A., Untch, M., and Smith, I. (2005) Trastuzumab after adjuvant chemotherapy in HER2-positive breast cancer. *N. Engl. J. Med. 353*, 1659–1672.

(21) Bange, J., Zwick, E., and Ullrich, A. (2001) Molecular targets for breast cancer therapy and prevention. *Nat. Med. 7*, 548–552.

(22) Weissleder, R. (1999) Molecular imaging: exploring the next frontier. *Radiology 212*, 609–614.

(23) Cai, W., Gambhir, S., and Chen, X. (2005) Multimodality tumor imaging targeting integrin $\alpha v\beta 3$. *Bio. Techniques 39*, S6–S17.

(24) Christophe, M. D., Abhijit, D., Andreas, M. L., Patrick, L. C., Pritha, R., Arion, F. C., and Sanjiv, S. G. (2007) Multimodality imaging of tumor Xenografts and metastases in mice with combined small-animal PET, small-animal CT, and bioluminescence imaging. *J. Nucl. Med. 48*, 295–303.

(25) Wang, Y., Nakamura, K., Liu, X., Kitamura, N., Kubo, A., and Hnatowich, D. J. (2007) Simplified preparation via streptavidin of antisense oligomers/ carriers nanoparticles showing improved cellular delivery in culture. *Bioconjug. Chem. 18*, 1338–1343.

(26) Wang, Y., Liu, X., Chen, L., Cheng, D., Rusckowski, M., and Hnatowich, D. J. (2009) Tumor delivery of antisense oligomer using trastuzumab within a streptavidin nanoparticle. *Eur J. Nucl. Mol. Imaging 36*, 1977–1986.

BC100081H